

# Diffusion Magnetic Resonance Imaging: Its Principle and Applications

SUSUMU MORI\* AND PETER B. BARKER

Diffusion magnetic resonance imaging (MRI) is one of the most rapidly evolving techniques in the MRI field. This method exploits the random diffusional motion of water molecules, which has intriguing properties depending on the physiological and anatomical environment of the organisms studied. We explain the principles of this emerging technique and subsequently introduce some of its present applications to neuroimaging, namely detection of ischemic stroke and reconstruction of axonal bundles and myelin fibers. *Anat Rec (New Anat) 257:102–109, 1999.*

© 1999 Wiley-Liss, Inc.

**KEY WORDS:** brain imaging; magnetic resonance imaging; diffusion MRI; diffusion tensor imaging; stroke; fiber reconstruction

It is truly amazing to realize that more than two decades after the invention of magnetic resonance imaging (MRI),<sup>8</sup> this technology is still evolving with considerable speed. The technique of *diffusion-weighted imaging* (DWI) is one of the most recent products of this evolution. Briefly speaking, this approach is based on the measurement of Brownian motion of molecules. It has been long, but not widely known that nuclear magnetic resonance is capable of quantifying diffusional movement of molecules.<sup>17</sup> In the 1980s, a method that combines this diffusion measurement with MRI was introduced, which is now widely called *diffusion imaging*.<sup>18,10,9</sup> This technique can characterize water diffusion properties at each picture element (pixel) of an image. The first important application of diffusion MRI emerged at center stage of the MRI community in early 1990s when it was discovered that DWI can detect stroke

in its acute phase.<sup>14</sup> Around the same time, scientists had also noticed that there is a peculiar property of water diffusion in highly ordered organs such as brains.<sup>13,11,5,6,19</sup> In these organs, water does not diffuse equally in all directions, a property called *anisotropic diffusion*. For example, brain water diffuses preferentially along axonal fiber directions. We now believe that it is possible to use this diffusion property as a probe to study the structure of spatial order in living organs non-invasively. In this tutorial, We will explain the physical principles of this emerging technology and introduce its present applications.

## CONVENTIONAL MRI

Before explaining diffusion MRI, we will briefly go over principles of conventional MRI—proton density and  $T_2$ -weighted imaging—because they share some important analogies with diffusion MRI. In MRI, we usually observe water protons, because they are by far the dominant chemical species observable by magnetic resonance. MRI is an extraordinarily versatile technique because of its capability of producing various types of contrast in the images, or so-called, *weighting*. Water protons have characteristic MRI properties depending on their physical and chemical environments. Vari-

ous types of MRI techniques have been designed to use the difference in such MRI properties of water in different tissues to differentiate regions of interest.

In order to explain the concept of the conventional MRI, we use the analogy of a gyroscope (Fig. 1). In an MRI experiment, we first excite water protons in a sample (or human in our case) with the imposition of a strong magnetic field. This is similar to starting the rotation of millions of gyro-

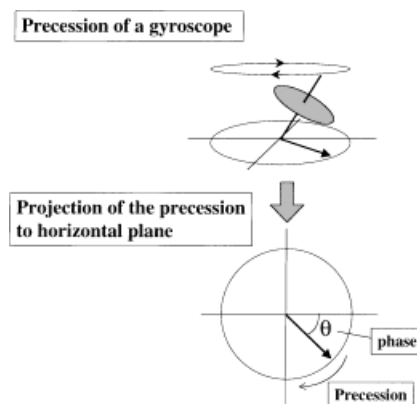


**Figure 1.** Analogy of MRI signal to a gyroscope. After excitation of protons in MRI, the signal behaves like a gyroscope that precesses at a fixed rate. If the position of the gyroscope is projected to a horizontal plane, such precession can be presented as a rotating vector. The position of the vector is called *phase*.

Drs. Mori and Barker are faculty members in the Department of Radiology, The Johns Hopkins University School of Medicine, Baltimore, Maryland.  
\*Correspondence to: Susumu Mori, Ph.D., Johns Hopkins University School of Medicine, Department of Radiology, 217 Traylor Bldg., 720 Rutland Ave., Baltimore, MD 21205. Fax: (410) 614-1948; E-mail: susumu@mri.jhu.edu

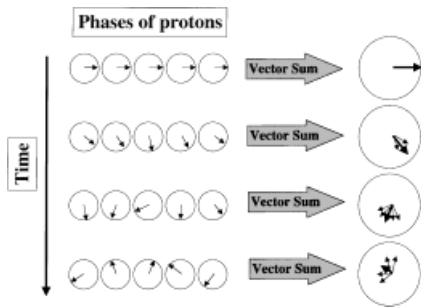


**Figure 2.** Mechanism of  $T_2$  relaxation. Phase of each proton is gradually randomized after excitation due to slightly different precession rates. As a result, the vector sum (indicated by thick arrows) decreases over the time, which means signal loss in MRI.

scopes simultaneously. The gyroscopes will start to precess, and it is this precession-equivalent of water protons that produces signals (electric currents in a receiver) in MRI. If the movement of the gyroscope is projected to a horizontal plane, the precession can be presented as a rotating vector as shown in Figure 1. The position of this vector is called the *phase*.

In a standard *proton density image*, the visual contrast is determined by the concentration of water, or the number of gyroscopes in our analogy. Namely, the more water in a given region, the brighter the region will appear. The more frequently used, but more difficult to understand, protocols generate so-called *relaxation-weighted* images, such as  $T_2$ -weighted images. After the excitation, there are

**Water protons have characteristic MRI properties depending on their physical and chemical environments. Various types of MRI techniques have been designed to use the difference in such MRI properties of water in different tissues to differentiate regions of interest.**

several mechanisms through which the signal eventually diminishes, or *relaxes*. The  $T_2$  relaxation can be explained by a loss of *coherence* or synchrony between the gyroscope rotations. Right after the excitation, all the gyroscopes have the same phase (Fig. 2). However, as time goes by, the phases of gyroscopes become randomized because each gyroscope precesses at slightly different speed due to various reasons such as local non-homogeneity of the magnetic field. Because what we observe is the vector sum with different phases, this randomization of the phase leads to the loss of signal in MRI, which is called  $T_2$  relaxation.

Depending on the location of water protons related, for example, to pathological conditions, the time required for  $T_2$  relaxation varies, resulting in different degrees of signal loss. This in turn can be used for the diagnosis of certain diseases. The exact mechanism that confers longer or shorter  $T_2$  relaxation is not completely understood. One thing we are sure of is that when water is in an environment where it can freely tumble (e.g., less viscosity or less macromolecules with which to interact), the relaxation tends to take longer. One typical example is the formation of edema, which leads to significant slowing of the relaxation and a prolonged  $T_2$ -weighted signal.

The  $T_2$  weighting can be obtained by inserting a *weighting period* in between the excitation and data acquisition (Fig. 3) and this time period (strictly speaking from the time point of excitation to the beginning of the acquisition) is called *echo time* (TE). Depending on the TE, the amount of  $T_2$  weighting varies. We can obtain a heavily weighted image by increasing TE, while the use of the shortest possible TE produces minimally  $T_2$ -weighted images. Examples of the lightly weighted (short TE) and heavily  $T_2$ -weighted (long TE) images are shown in Figure 4. Regions in the brain that have slow  $T_2$  relaxation show up bright, such as cerebrospinal fluid (CSF). White matter has faster  $T_2$  relaxation and consequently looks darker. The minimally  $T_2$ -weighted image in Figure 4a is referred as “proton density,” which means the image is not weighted by anything but water concentration (in other words, “proton density”).

### DIFFUSION WEIGHTING

Weighting of MRI by diffusion can also be explained using the analogy to the gyroscope. Just as the rate of the precession of the gyroscope is proportional to the strength of gravity, in MRI the rate of the precession is proportional to the strength of the magnet. For example, in a typical MRI magnet of 1.5 tesla (T), the rate of the precession is about 64 MHz. Because the strength of magnetic field is kept as homogeneous as possible, this precession rate is also very homogeneous across the magnet. This homogeneity can be disturbed linearly by using a so-called pulsed field gradient. The strength (slope) of the gradient, its direction, and the time period can be controlled. As an example, Figure 5 shows a diagram of an *x gradient*. As a result of this gradient application, protons start to precess at a different rate along the x-axis. With an analogy to the  $T_2$  relaxation process (Fig. 2), such differences in the precession rate lead to dispersion of the phase and signal loss (Fig. 6). However, if another gradient pulse is subsequently applied with the same direction and time period but of opposite magnitude, such dispersion can be *refocused* or re-phased, therefore, the first gradient is called the *dephasing gradient* and the second one the *rephasing gradient*.

From Figure 6, it can be understood that this refocusing can not be perfect if the protons moved in between a pair of the gradient applications. Thus, by applying a pair of gradient pulses after the excitation and before the data acquisition, we can sensitize the image (make the resultant image sensitive)

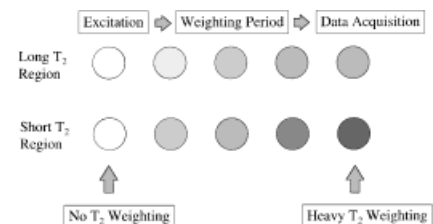


**Figure 3.** Mechanism of  $T_2$  weighting. By inserting a *waiting period* in between excitation and data acquisition, we can obtain relaxation weighting. For  $T_2$  weighting, a scheme called *spin-echo* is inserted (in this case, the spin-echo time is identical to the  $T_2$ -weighting period). The length of the inserted element determines the degree of weighting. Gray intensity in circles depicts relative image intensity.

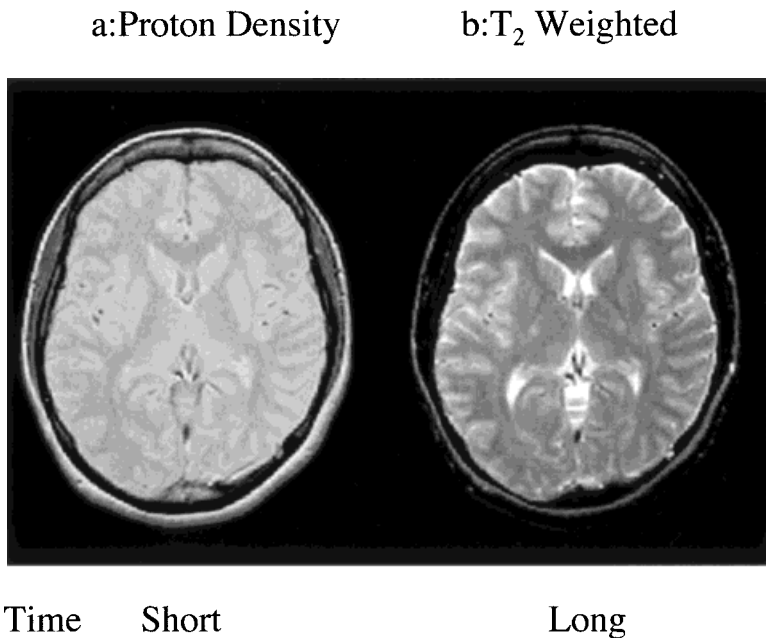


**Figure 4.** Examples of proton density (a) and T<sub>2</sub> (b) weighted images. Echo time for proton density was 5 ms and that for T<sub>2</sub> weighted image was 80 ms. Repetition time was 3 s for both images.

to motional processes such as flow or diffusion. The amount of the diffusional signal loss by the gradient application is known to obey an equation

$$\frac{S}{S_0} = e^{-\gamma^2 G^2 \delta^2 (\Delta - \delta/3) D} = e^{-bD}$$

where  $S_0$  is the signal intensity without the diffusion weighting (no gradient application) and  $S$  is the signal with the gradient application (Fig. 7).  $D$  is a diffusion constant. The equation indicates that the higher the diffusion constant, the larger the signal loss. The parameter  $\gamma$  is a nuclear constant called gyromagnetic ratio. It is intuitively understandable that the amount of signal loss depends on the time between the two pulses indicated by  $\Delta$ , because there is more time for water molecules to diffuse and, thus, the refocusing of the precessing protons is less perfect. Signal loss is also larger if the gradient pulses are stronger ( $G$ ) and/or longer ( $\delta$ ). Most commonly, we change the strength of the gradients to obtain various amounts of the diffusion weighting.

The result of a DWI experiment on a human brain is shown in Figure 8. It can be seen that signal intensity decreases as gradient strength increases and that the extent of the signal decay

depends on the diffusion constants of brain water. For example, signal from the cerebrospinal fluid (CSF) region (indicated by a white arrow in Figure 8) decays faster and therefore gives a “darker” image than that of brain matter. Although these diffusion-weighted images are useful, their absolute inten-

sity or contrast is not always a direct indicator of the diffusion constant at each pixel of the image. This is because DWI are affected by not only the degree of diffusion weighting ( $b$ -value dependent), but also other contrasting mechanisms, such as T<sub>2</sub>, and/or proton density. To appreciate the amount of water diffusion, the degree of the signal decay (or the slope of the decay) is more important than the absolute intensity of the images. Recalling Figure 7, if such signal decay ( $S(b)$ ) is plotted in logarithmic scale, diffusion constant at each pixel can be obtained from the slope. The calculated diffusion constants at each pixel can then be mapped to create an image called an *apparent diffusion constant* (ADC) image (Fig. 8).

### DIFFUSION MRI CAN DETECT STROKE IN ITS ACUTE PHASE

In 1991, it was found that the ADC of brain water drops drastically in the event of ischemia.<sup>14</sup> Although the exact mechanism of the drop is still not known, it is almost certain that the bulk of the effect is related to the breakdown of membrane potential. Because this technique is one of the few radiological techniques that can detect stroke in its acute phase, the impli-

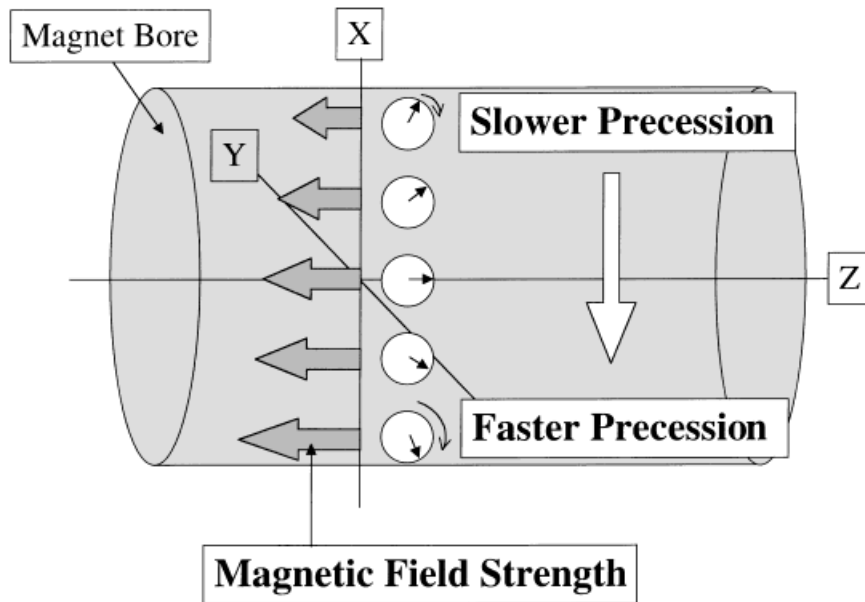


**Figure 5.** An example of an x-gradient. The direction along the magnet bore is defined as z, along which the main the magnetic field aligns. Gradient units introduce linear magnetic field inhomogeneity with a specified time period, magnitude, and direction. As a result, the precession rates vary in the sample depending on the position of the protons.

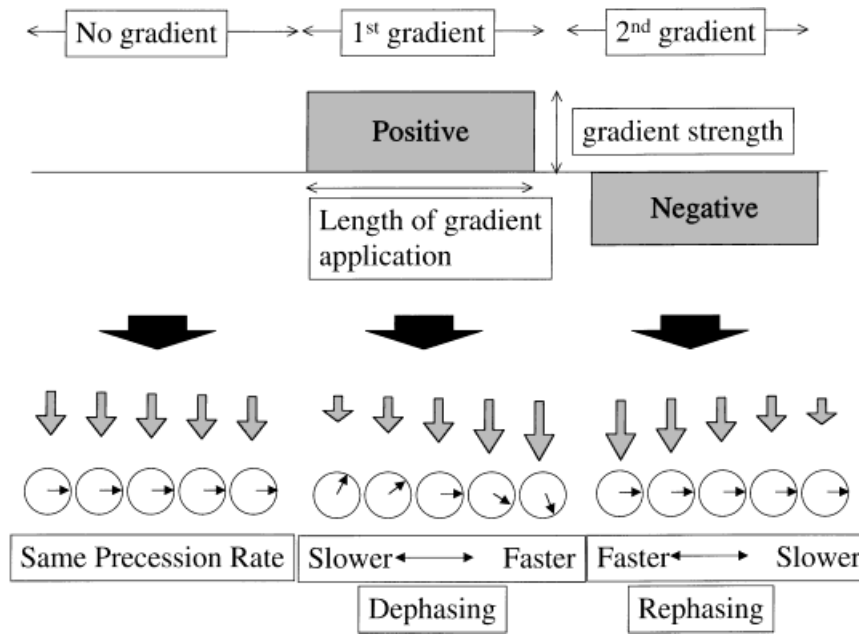


**Figure 6.** Gradient diagram (upper row) and signal phases (lower row) under application of a gradient. The length of gray arrows indicates the strength of the magnetic field that is non-uniform during the application of the gradients. After the first gradient application, signals lose their uniform phase (dephase) because each proton starts to precess at different rates depending on its position in space. Such a gradient application is indicated by boxes in the diagram representing duration and strength. After the second field application of opposite magnitude, the system restores uniform phase (rephase). This rephasing is complete only when spins do not move by Brownian motion (viz., diffuse) during the time in between the two applications of the gradient. The less complete the rephasing, the more signal loss results.

cation is significant. An example of the ADC drop is shown in Figure 9a.

**MEASURED DIFFUSION CONSTANT DEPENDS ON A DIRECTION OF THE MEASUREMENT**

By the time the ADC drop due to ischemia was reported, researchers had also noticed that there was a strong contrast in the ADC map of brains, which varies depending on the direction of the measurement.<sup>13,11,5,6,19</sup> This effect is demonstrated in Figure 9b-d. Note that MRI can measure molecular diffusion along any desired directional axis by using three independent gradient units that are orthogonal each other (*x*, *y*, and *z*, see Fig. 5). It can be seen that the orientation-dependent contrast is so great in Figure 9b-d, that the location of ischemia, compared to artifactual signals, can no longer be easily differentiated.

It is now known that this orientation-dependent contrast is generated by

*diffusion anisotropy*, in other words, water diffusion has directionality.<sup>3</sup> This concept is explained in Figure 10. When water is freely diffusing (Fig. 10a), it diffusion is isotropic (no directionality) and the measured ADC does not depend on the axis of the gradient application. However, water in living systems is often contained in very ordered structures that restrict its diffusion along certain axes. An example is shown in Figure 10b in which a water molecule is confined in a cylindrically shaped tube. In this case, a diffusion constant measured along the *z* axis is larger than those along *x* and *y*. In practice, such an ordered biological structure does not usually align to the physical coordinate, *x*, *y*, and *z* (see Fig. 10c) defined by orientation of an MRI scanner. In this case, what we measure using *x*, *y*, or *z* gradients is diffusion along an oblique angle with respect to the ordered structure.

From this example, it follows that the result of diffusion measurement along an axis depends on the orienta-

tion of the object in anisotropic media. Therefore, anisotropic diffusion can not be represented by one diffusion constant. We can fully characterize such a diffusion property by a  $3 \times 3$  tensor, called *diffusion tensor* ( $\overline{\overline{D}}$ )<sup>12,13</sup>

$$\overline{\overline{D}} = \begin{bmatrix} D_{xx} & D_{xy} & D_{xz} \\ D_{yx} & D_{yy} & D_{yz} \\ D_{zx} & D_{zy} & D_{zz} \end{bmatrix}$$

When a diffusion measurement is made along the *x*, *y*, or *z* axis, what we measure is  $D_{xx}$ ,  $D_{yy}$ , or  $D_{zz}$  respectively. The meaning of this diffusion tensor can be more easily understood using so-called diffusion ellipsoids (Fig. 10, middle row). In an isotropic environment, the diffusion tensor has only diagonal elements ( $D_{xx}$ ,  $D_{yy}$ , and  $D_{zz}$ ), all of which have the same value (Fig. 10a). Thus, the system can be characterized by only one value ( $D$ ) and the diffusion ellipsoid is spherical (the diffusion constant  $D$  is the diameter of the sphere). In an anisotropic environment, the ellipsoid is elongated. We call the longest, middle, and shortest axes of this *ellipsoid principal axes* and the three diffusion constants along the axes  $\lambda_1$ ,  $\lambda_2$ , and  $\lambda_3$ . When the principal axes happen to align to our physical coordinate *x*, *y*, and *z*, we can directly measure  $\lambda_1$ ,  $\lambda_2$ , and  $\lambda_3$  as shown in Figure 10b. In practice, they are almost never aligned (Fig. 10c) and the diffusion tensor has nine non-zero values. Because  $D_{xx}$ ,  $D_{yy}$ , and  $D_{zz}$  values change as the orientation of the object changes, so does the measured diffusion constant using *x*-, *y*-, and *z*-gradient axes.

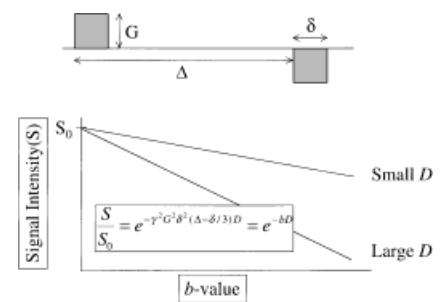


**Figure 7.** Relationship between gradient application, signal loss, and diffusion constant ( $D$ ). Gradient strength ( $G$ ), duration ( $\delta$ ), and separation ( $\Delta$ ) affect the signal. When  $b$ -value ( $=\gamma^2 G^2 \delta^2 (\Delta - \delta/3)$ ) is plotted against the signal decay, the slope represents the diffusion constant.

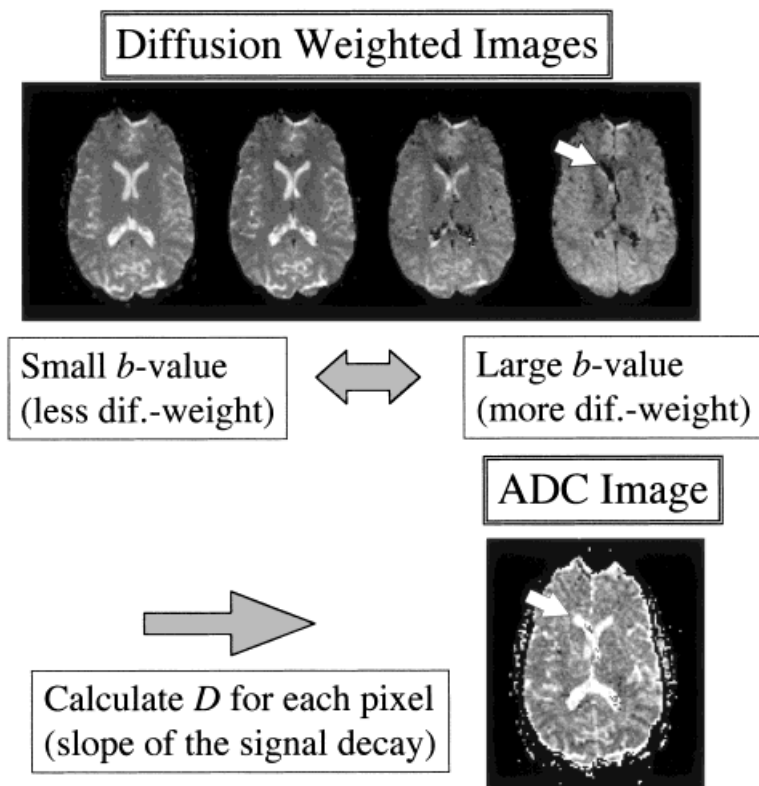


**Figure 8.** An example of a diffusion-weighted and an apparent diffusion constant (ADC) image of a human brain. From a series of diffusion-weighted images with different  $b$ -values, an ADC image can be calculated. Only from ADC can we purely appreciate diffusion properties of water at each pixel.

#### CONTRAST CAUSED BY THE ANISOTROPY EFFECT IS NOT DESIRABLE FOR STROKE DETECTION

In light of the previous discussion, it should be more clear why the ADC maps of a human brain in Figures 9b–d can look so different depending on the orientation of the diffusion measurement. For example, in Figure 9b—where diffusion was measured along the  $x$ -axis—the bright part of the brain has fibers oriented parallel to  $x$ , whereas those in the dark region are oriented perpendicular to it. This strong contrast due to the anisotropy effect is unwanted for the detection of the stroke.

One of the most intriguing properties of the tensor is that certain combinations of the diffusion tensor elements are not susceptible to contrast caused by this anisotropy effect. The simplest and most widely used combination is the so-called *trace* of the tensor ( $D_{xx} + D_{yy} + D_{zz}$ ).<sup>22</sup> In other words, if three ADC maps generated

using  $x$ -,  $y$ -, and  $z$ -gradient axes are added all together, the image contrast is insensitive to the anisotropy effect in any one axis and no difference between gray and white matter remains. An example of this trace image is shown Figure 9a. It can be seen that entire brain now has a very homogenous ADC and a stroke region is easily discerned as a dark patch (indicated by the white arrows).

#### STUDY OF BRAIN FIBER STRUCTURES FROM THE ANISOTROPY EFFECT

While anisotropy is an unwanted property of water diffusion for the detection of stroke, it carries very intriguing information about brain neuronal structures. Although we still do not know exactly which neuronal structures confer the diffusion anisotropy,<sup>7,4</sup> there is much evidence suggesting that myelination and/or protein fiber bundles of axons are the most likely source. For example, there is higher anisotropy in white matter than gray matter and in adult brains compared with those of newborns. It follows that the DWI technique should provide us

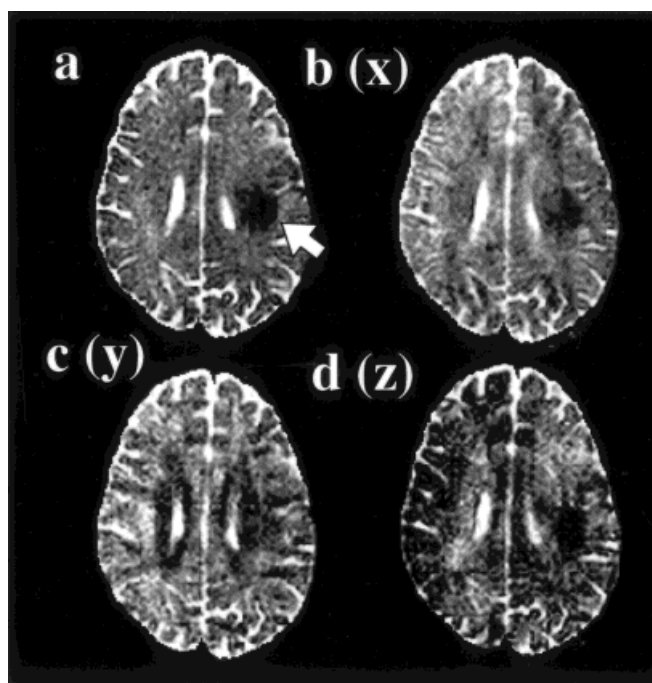


**Figure 9.** ADC images of a human brain with stroke. White arrow indicates area of darkness, corresponding to damage from stroke. The image shown in a is a *trace* image which is obtained by adding three ADC images recorded using  $x$ -gradient (b),  $y$ -gradient (c), and  $z$ -gradient (d). There is strong contrast in the ADC images measured along a single axis (b–d), which is due to the presence of water molecules diffusing along axonal fibers. This contrast is removed in a. (Figure reproduced from Ulug et al.<sup>21</sup> with permission.)

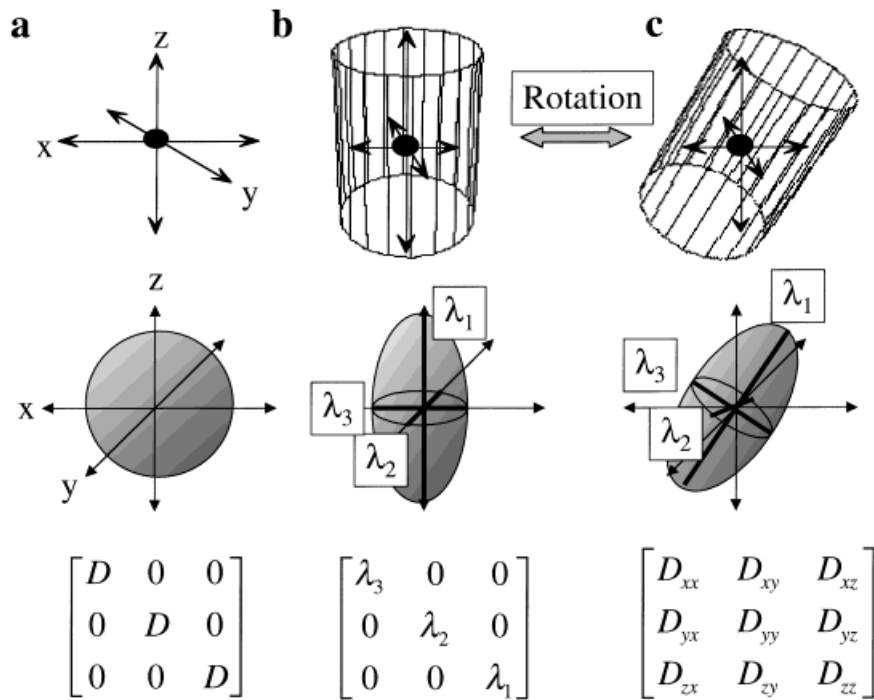


**Figure 10.** Relationship between anisotropic diffusion (upper row), diffusion ellipsoids (middle row), and diffusion tensor (bottom row). When environment is isotropic (a), water diffuses equivalently in all directions. The diffusion ellipsoid of this system is spherical and can be depicted by one diffusion constant,  $D$ . When the environment is anisotropic, e.g. cylindrical (b,c), water diffusion has directionality. The diffusion ellipsoid of water in a cylinder is elongated and has three principal axes,  $\lambda_1$ ,  $\lambda_2$ , and  $\lambda_3$ . To fully characterize such a system,  $3 \times 3$  tensor is needed and the values of the nine elements depend on the orientation of the principal axes.

with entirely new information about axonal fiber structures, which no other radiological technique has been able to previously.

To investigate axonal structures, we first have to fully characterize the diffusion ellipsoid at each pixel. The most intuitive method of characterization is to measure diffusion constants (or create ADC maps) along numerous directions, from which we can deduce the shape of the ellipsoids. This can be achieved by using three gradient units. For example, if  $x$  and  $y$  gradients are applied simultaneously, diffusion along a direction 45 degrees from the  $x$  and  $y$  axis can be measured. In this way, we can measure diffusion along any desired angles. Tensor theory tells us if we measure the diffusion constant along six independent axes, we can calculate the complete shape of the diffusion ellipsoid.<sup>3,1,2,20</sup> Namely, we can obtain  $\lambda_1$ ,  $\lambda_2$ , and  $\lambda_3$  and their directions.

From this characterization of the diffusion ellipsoid at each pixel, we can now obtain two important parameters. One is called the *anisotropy in-*

*dex*, which indicates how anisotropic the diffusion is—or in other words, how elongated the ellipsoid is.<sup>15</sup> This indicates how packed and/or ordered the axonal fibers are in each pixel. The simplest method to calculate this is to take a ratio of  $\lambda_1$  and  $\lambda_3$ , which are diffusion constants along the longest and shortest axes of a diffusion ellipsoid. However, this method does not have good statistical stability and many more elaborate ways to characterize the anisotropy have been postulated.<sup>15</sup> One example is shown in Figure 11b. Compared to conventional  $T_2$  weighted images (Fig. 11a), Figure 11b depicts much more detailed structures of white matter tracts. This is understandable because water diffusion anisotropy is a more direct indicator of the presence of packed fibers than  $T_2$  weighting, which is affected by many other parameters. It has been reported that the anisotropy index of white matter increases during brain development possibly due to the process of myelination.<sup>16,23</sup> Thus, there is an expectation that this technique will be a sensitive

indicator of myelination abnormalities.

Besides the anisotropy index, the second important parameter we can obtain is the direction of axonal fibers. Assuming water tends to diffuse along fibers, this can be achieved by identifying the direction of the longest axis of diffusion ellipsoids in a given image section. An example is shown in Figure 11c. In this figure, some prominent fibers can be easily appreciated,

**In the near future, we believe that the technique of 3D-diffusion MRI reconstruction will be an important tool used to observe white matter tracts of live humans for the study of connectivity of brain functional centers, brain development, and white matter diseases.**

which are indicated by color-coding. Once we know the fiber direction at each pixel, it then should be possible to reconstruct three-dimensional (3D) fiber structures by connecting their passage through multiple image slices. We have pursued this goal of brain fiber mapping by acquiring high-resolution 3D diffusion MRI data using fixed rat brains.<sup>12</sup> An example of such a 3D reconstruction is shown in Figure 11d. This kind of information on white matter tracts was previously obtained only by invasive *in vivo* experiments such as tracer techniques.

In the near future, we believe that the technique of 3D-diffusion MRI reconstruction will be an important tool used to observe white matter tracts of live humans for the study of connectivity of brain functional centers, brain development, and white matter diseases.

**IN SUMMARY**

In this article, we introduced the concept of diffusion MRI and its applica-

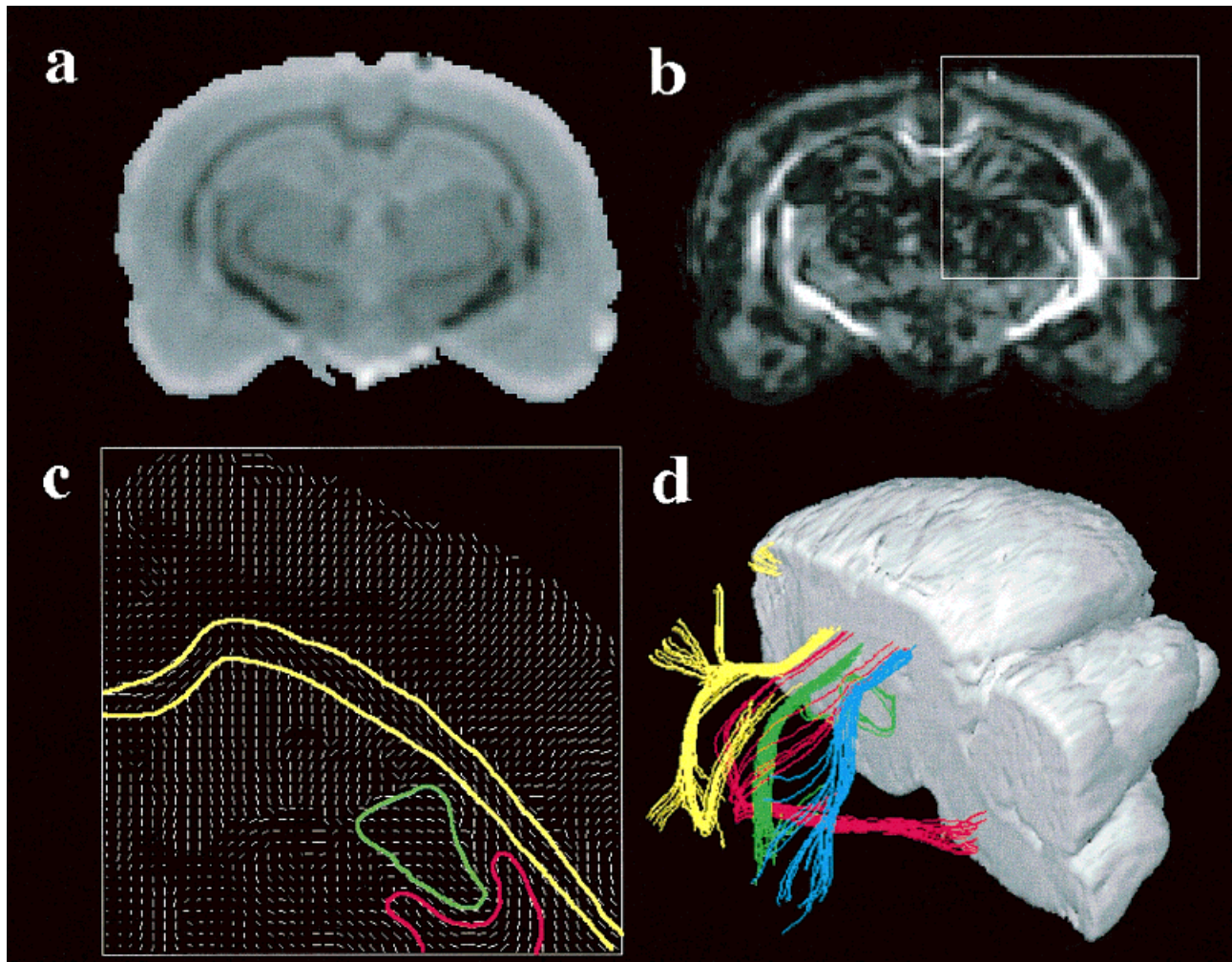


**Figure 11.** Results of the diffusion tensor imaging. A  $T_2$  weighted image (a) and an anisotropy image (b) from a same slice are shown. In b, highly anisotropic regions are light. The light regions in b mostly overlap with dark regions in the  $T_2$  weighted image (a), which is white matter. However, the anisotropy map (b) reveals much more detailed information on fiber tracts. Fiber directions in a region indicated by the box in (b) are shown in c. Prominent axonal projections such as corpus callosum (yellow), fimbria (green), and internal capsule (red) can be easily seen. From 3D diffusion tensor imaging, 3D structures of these projections can be reconstructed (d). The color-coding in d is the same as c except for the splenium of the corpus callosum (blue). (Figure reproduced from Mori et al.<sup>12</sup> with permission.)

tions. The technique is already widely used for the study of stroke. A newly emerging application is *diffusion tensor imaging*, which allows us to study axonal brain fiber structures. For both techniques, it is very important to realize that water diffusion in living system is often anisotropic.

#### ACKNOWLEDGMENTS

This research was funded in part by a grant from the American Federation of Aging Research, the Whitaker Foundation, and NIH (RO3 HD37931-01). I would like to thank Dr. Peter van Zijl

for giving suggestions and critically reviewing the manuscript.

#### LITERATURE CITED

1 Bassler PJ, Mattiello J, LeBihan D. 1992. Diagonal and off-diagonal components of the self-diffusion tensor: their relation to and estimation from the NMR spin-echo signal. Berlin.

2 Bassler PJ, Mattiello J, Le Bihan D. 1994. MR diffusion tensor spectroscopy and imaging. *Biophys J* 66:259–267.

3 Bassler PJ, Mattiello J, LeBihan D. 1994. Estimation of the effective self-diffusion tensor from the NMR spin echo. *J Magn Reson B* 103:247–254.

4 Beaulieu C, Allen PS. 1994. Determinants of anisotropic water diffusion in nerves. *Magn Reson Med* 31:394–400.

5 Chenevert TL, Brunberg JA, Pipe JG. 1990. Anisotropic diffusion in human white matter: demonstration with MR technique in vivo. *Radiology* 177: 401–405.

6 Doran M, Hajnal JV, van Bruggen N, King MD, Young IR, Bydder GM. 1990. Normal and abnormal white matter tracts shown by MR imaging using directional diffusion weighted sequences. *J Comput Assist Tomogr* 14:865–873.

7 Henkelman R, Stanisz G, Kim J, Bronskill M. 1994. Anisotropy of NMR properties of tissues. *Magn Reson Med* 32:592–601.

- 8** Lauterbur PC. 1973. Image formation by induced local interactions: examples employing nuclear magnetic resonance. *Nature* 243:190.
- 9** Le Bihan D, Breton E, Lallemand D, Grenier P, Cabanis E, Laval-Jeantet M.. 1986. MR imaging of intravoxel incoherent motions: application to diffusion and perfusion in neurologic disorders. *Radiology* 161:401-407.
- 10** Merboldt KD, Hanicke W, Frahm J. 1985. Self-diffusion NMR imaging using stimulated echoes. *J Magn Reson* 64:479-486.
- 11** Moonen CTW, Pekar J, de Vleeschouwer MH, van Gelderen P, van Zijl PCM, DesPres D. 1991. Restricted and anisotropic displacement of water in healthy cat brain and in stroke studied by NMR diffusion imaging. *Magn Reson Med* 19:322-327.
- 12** Mori S, Crain BJ, Chacko VP, van Zijl PCM. 1999. Three dimensional tracking of axonal projections in the brain by magnetic resonance imaging. *Ann Neurol* 45:265-269.
- 13** Moseley ME, Cohen Y, Kucharczyk J, Mintorovitch J, Asgari HS, Wendland MF, Tsuruda J, Norman D. 1990. Diffusion-weighted MR imaging of anisotropic water diffusion in cat central nervous system. *Radiology* 176:439-445.
- 14** Moseley ME, Kucharczyk J, Mintorovitch J, Cohen Y, Kurhanewicz J, Derugin N, Asgari H, Norman D. 1990. Diffusion-weighted MR imaging of acute stroke: correlation with T2-weighted and magnetic susceptibility-enhanced MR imaging in cats. *Am J NeuroRad* 11:423-429.
- 15** Pierpaoli C, Basser PJ. 1996. Toward a quantitative assessment of diffusion anisotropy. *Magn Reson Med* 36:893-906.
- 16** Sakuma H, Nomura Y, Takeda K, Tagami T, Nakagawa T, Tamagawa Y, Ishii Y, Tshukamoto T. 1991. Adult and neonatal human brain: diffusional anisotropy and myelination with diffusion-weighted MR imaging. *Radiology* 180:229-233.
- 17** Stejskal EO, Tanner JE. 1965. Spin diffusion measurement: spin echoes in the presence of a time-dependent field gradient. *J Chem Phys* 42:288.
- 18** Taylor DG, Bushell MC. 1985. The spatial mapping of translational diffusion coefficients by the NMR imaging technique. *Phys Med Biol* 30:345-349.
- 19** Turner R, LeBihan D, Maier J, Vavrek R, Hedges LK, Pekar J. 1990. Echo-planar imaging of intravoxel incoherent motions. *Radiology* 177:407-414.
- 20** Ulug AM, Bakht O, Bryan RN, van Zijl PCM. 1996. Mapping of human brain fibers using diffusion tensor imaging. New York.
- 21** Ulug AM, Beauchamp N, Jr, Bryan RN, van Zijl PC. 1997. Absolute quantitation of diffusion constants in human stroke. *Stroke* 28:483-490.
- 22** van Gelderen P, DesPres D, van Zijl PCM, Moonen CTW. 1994. Water diffusion and acute stroke. *Magn Reson Med* 31:154-163.
- 23** Wimberger D, Roberts T, Barkovich A, Prayer L, Moseley M, Kucharczyk Z. 1995. Identification of "premyelination" by diffusion-weighted magnetic resonance imaging. *J. Comput. Assist. Tomogr.* 19:28-33.